14 May 2026

A Decoupling Strategy for Position-Controlled Access to 1,3-Disubstituted Saturated Frameworks

Lohitha H. Ramu, Devagi Narasimman, Jayasish Ghosh, Vignesh Palani

Abstract

The three-dimensional architecture and precise placement of functional groups critically influence the performance of drugs and functional materials, yet positional control on saturated carbocycles remains limited1–3. Framework editing, rather than de novo synthesis, offers an attractive strategy for direct site-selective synthesis of functionalized carbocycles. In particular, functional group translocation—migrating an existing substituent within a molecular framework without altering its core structure—has emerged as a powerful approach to access valuable substitution patterns in saturated systems4. However, its development has largely been confined to 1,2-5–10 and 1,4-migrations11,12. Here, we report a general and conceptually distinct platform for formal transannular 1,3-migration of aroyl groups across saturated carbocycles, enabling precise access to 1,3-disubstituted frameworks. This strategy proceeds via a neutral bicyclic intermediate generated by Norrish–Yang photocyclization, which is then oxidatively cleaved with hydrogenatom trapping. A distinctive feature is the coexistence of oxidant Mn(OAc)3 and a thiol reductant without their mutual quenching, enabling independent downstream reactivity. By decoupling cyclization from the migration event, this approach overcomes kinetic constraints that have historically precluded 1,3-translocation13. Broadly applicable to both radical and ionic pathways, this method enables ring expansion, scaffold hopping, distal editing through iterative translocation, and stereospecific modification of chiral substrates.

Title: A Decoupling Strategy for Position-Controlled Access to 1,3-Disubstituted Saturated Frameworks

Authors Lohitha H. Ramu, Devagi Narasimman, Jayasish Ghosh, Vignesh Palani*

Affiliations Department of Organic Chemistry, Indian Institute of Science, Bengaluru 560012.

*Correspondence to: vpalani@iisc.ac.in

Abstract: The three-dimensional architecture and precise placement of functional groups critically influence the performance of drugs and functional materials, yet positional control on saturated carbocycles remains limited[1–3]. Framework editing, rather than de novo synthesis, offers an attractive strategy for direct site-selective synthesis of functionalized carbocycles. In particular, functional group translocation—migrating an existing substituent within a molecular framework without altering its core structure—has emerged as a powerful approach to access valuable substitution patterns in saturated systems[4]. However, its development has largely been confined to 1,2-[5–10] and 1,4-migrations[11,12]. Here, we report a general and conceptually distinct platform for formal transannular 1,3-migration of aroyl groups across saturated carbocycles, enabling precise access to 1,3-disubstituted frameworks. This strategy proceeds via a neutral bicyclic intermediate generated by Norrish–Yang photocyclization, which is then oxidatively cleaved with hydrogen-atom trapping. A distinctive feature is the coexistence of oxidant $Mn(OAc)_3$ and a thiol reductant without their mutual quenching, enabling independent downstream reactivity. By decoupling cyclization from the migration event, this approach overcomes kinetic constraints that have historically precluded 1,3-translocation[13]. Broadly applicable to both radical and ionic pathways, this method enables ring expansion, scaffold hopping, distal editing through iterative translocation, and stereospecific modification of chiral substrates.

Main Text

Saturated carbocycles are common motifs in natural products, with their physicochemical properties and biological activity strongly dependent on the nature and position of appended functional groups (FGs). Despite sustained interest, methods enabling precise positional control of FGs on saturated carbocycles remain limited[14]. Conventional approaches (Fig. 1A), including convergent coupling and cyclization, represent logical entry points but are constrained by stringent requirements for polarity matching, steric differentiation, and precise geometric preorganization of precursors[15,16]. Alternatively, post-assembly modification of cyclic frameworks—most commonly via directing-group-assisted sp^3 C–H activation—has been explored[17]. However, selective installation of FGs at remote sp^3 C–H sites in the absence of directing groups remains a formidable challenge due to the inertness of aliphatic C–H bonds and the high degree of site equivalence, which together impede regio- and stereochemical control[18,19].

A conceptually distinct solution is intramolecular FG translocation, wherein an existing substituent is repositioned within a molecular framework without otherwise perturbing its structure. This peripheral skeletal editing strategy[4] enables direct access to synthetically challenging substitution patterns and is particularly attractive for late-stage diversification, as substituent relocation can generate analogues with distinct biological profiles[20,21]. While recent advances have enabled proximal 1,2-FG translocation across diverse scaffolds[5–8], methods for distal FG migration remain

scarce. Recently, Xu and co-workers disclosed a dynamic kinetic strategy enabling 1,4-cyano group translocation in both acyclic and cyclic systems (Fig. 1B, left)[11]. This approach proceeds through reversible, non-selective cleavage of multiple similar C–H bonds followed by site-selective radical addition. Preferential formation of kinetically favored five-membered-ring intermediates enforces 1,4-selectivity, rendering alternative distal migrations disfavored. Building on this concept, Wendlandt and co-workers demonstrated transannular 1,4-acyl migration in cycloheptyl systems via a kinetically preferred [3.2.1] bicyclic intermediate[12]. In a related advance, 1,2-boryl migration across saturated frameworks was accomplished under conditions governed by dynamic kinetic control[9,10].

The inherent selectivity limitations of dynamic kinetic protocols highlight the need for fundamentally different strategies to access alternative modes of distal FG translocation. Herein, we describe a dual-phase, position-controlled translocation strategy (Fig. 1B, right) that proceeds through an initial directed sp^3 C–H bond cleavage followed by radical recombination to form a neutral intermediate (*cyclization phase*). Subsequent β-scission, coupled with hydrogen-atom trapping (*cleavage phase*), enables effective migration of the FG to a targeted position. A defining feature of this approach is deliberate decoupling of cyclization and cleavage, which prevents formation of kinetically unstable cyclic radical intermediates. Importantly, irreversibility associated with neutral intermediate formation enables FG migration pathways that are not governed by kinetic alignment.

Under conventional dynamic kinetic control, assembly of cyclobutyl or cycloheptyl radical intermediates required for 1,3- or 1,6-translocation is strongly disfavored. Consistent with this limitation, Zhu and co-workers demonstrated that even site-selective radical generation at the C3 or C6 position fails to yield productive cyclization[22,23], underscoring intrinsic challenges associated with radical-mediated access to 1,3- or 1,6-FG translocation. In contrast, by decoupling cyclization from cleavage, the position-controlled platform renders these otherwise inaccessible translocations feasible via neutral cyclic intermediates.

As an initial demonstration of this strategy, we targeted 1,3-translocation of aroyl groups in saturated cyclohexyl systems (Fig. 1C). This transformation exploits an underexplored transannular Norrish–Yang cyclization[24] to generate a strained yet neutral bicyclo[3.1.1] intermediate (*cyclization phase*), which subsequently undergoes selective cleavage to afford the net 1,3-translocated product (*cleavage phase*). Beyond proof of concept, this method provides direct access to 1,3-disubstituted cyclohexyl derivatives, motifs prevalent in biologically active molecules[25,26]. Although the aroyl group was selected for its ability to participate in photocyclization and promote selective Cγ–H bond cleavage, its synthetic and biological relevance is equally significant. Aroyl moieties are versatile intermediates readily diversified through classical carbonyl transformations and transition-metal-catalyzed processes[27]. Moreover, in bioactive compounds such as paclitaxel, aroyl positioning correlates directly with biological activity[28], underscoring the value of controlled aroyl migration. This fully atom-economical transformation proceeds with high regioselectivity across a broad range of saturated frameworks, providing efficient access to diverse 1,3-substituted architectures. A predictive model is established to guide substrate design and to facilitate extension of this strategy to a wide range of synthetic applications, supported by detailed mechanistic insights.

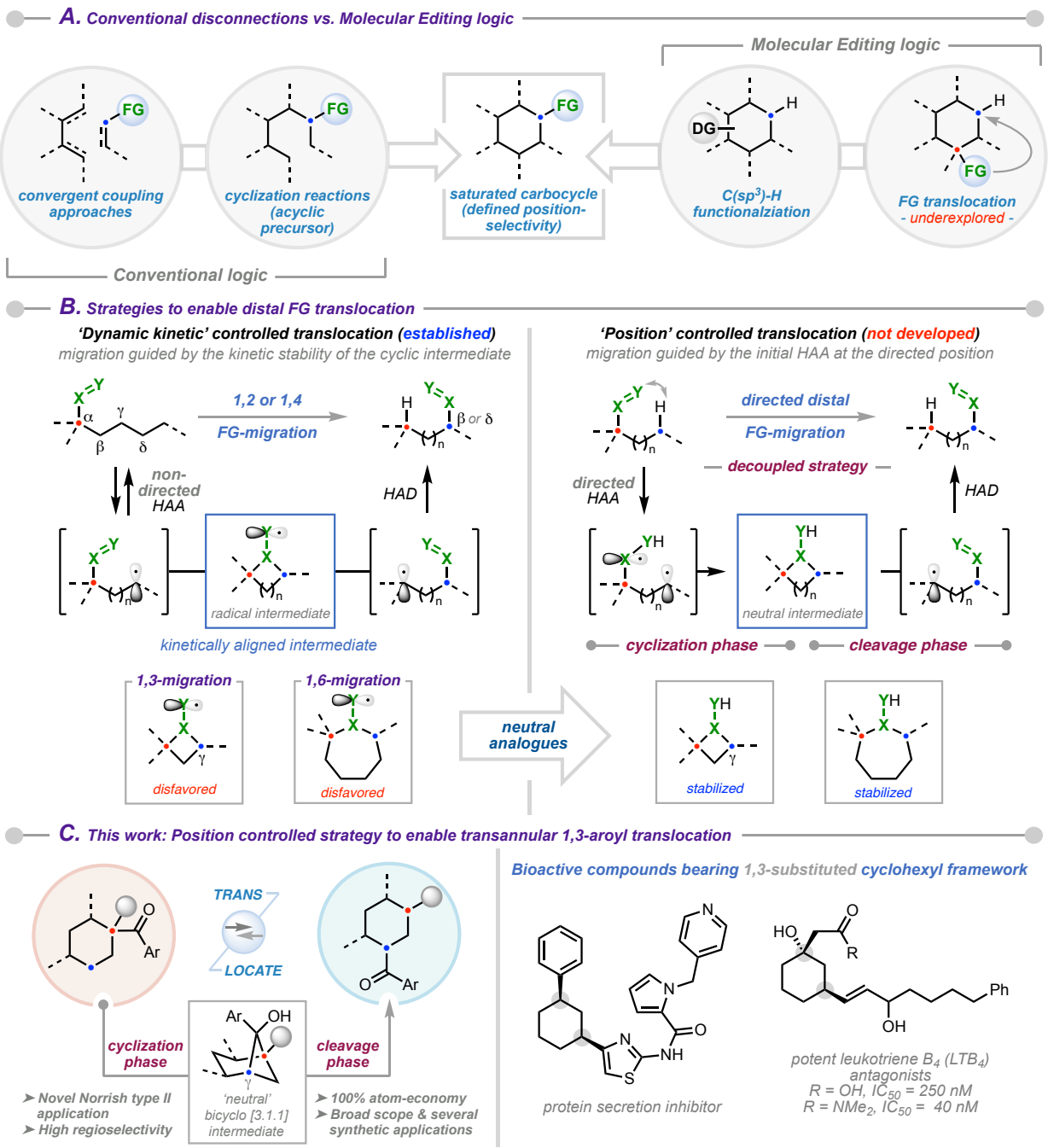

Fig. 1. Conceptual overview and importance of functional group translocation strategies. (A) Comparison of conventional approaches and Molecular Editing logic for achieving positional control on saturated carboxylic frameworks. (B) Constraints of radical-mediated pathways and the value of a decoupling strategy in enabling position-selective functional group translocations. FG, functional group; HAA, hydrogen atom abstraction; HAD, hydrogen atom donation; X=Y, hypothetical atoms on the π-bond (C) This work: a decoupled, position-controlled approach that enables transannular 1,3-migration of aroyl groups, providing access to biologically potent 1,3-disubstituted cyclohexyl framework.

We initiated our investigation by synthesizing 1-benzoyl-1-methylcyclohexane (**1a**) as a model substrate (Fig. 2A). Upon irradiation, we targeted the symmetry-forbidden, lower-energy n → π* transition to access the triplet state of **1a**. When the aroyl group adopts a pseudoaxial orientation,

the oxygen-centered radical engages in a Norrish type II 1,5-hydrogen atom transfer (HAT) with the proximal C3-axial C–H bonds, forming the 1,4-diradical intermediate **1ab**. Subsequent radical recombination furnishes the cyclobutyl intermediate **1c**. Guided by a few prior reports[29,30] and UV-visible absorption spectra of **1a** (λ_{max} = 315 nm), irradiation in *tert*-butanol with a 370-nm LED lamp yielded **1c** in 66%. Notably, a high-intensity medium-pressure Hg lamp promoted decomposition (55% yield of **1c**), whereas a lower-energy 390-nm LED lamp afforded **1c** in 58% yield over longer reaction times.

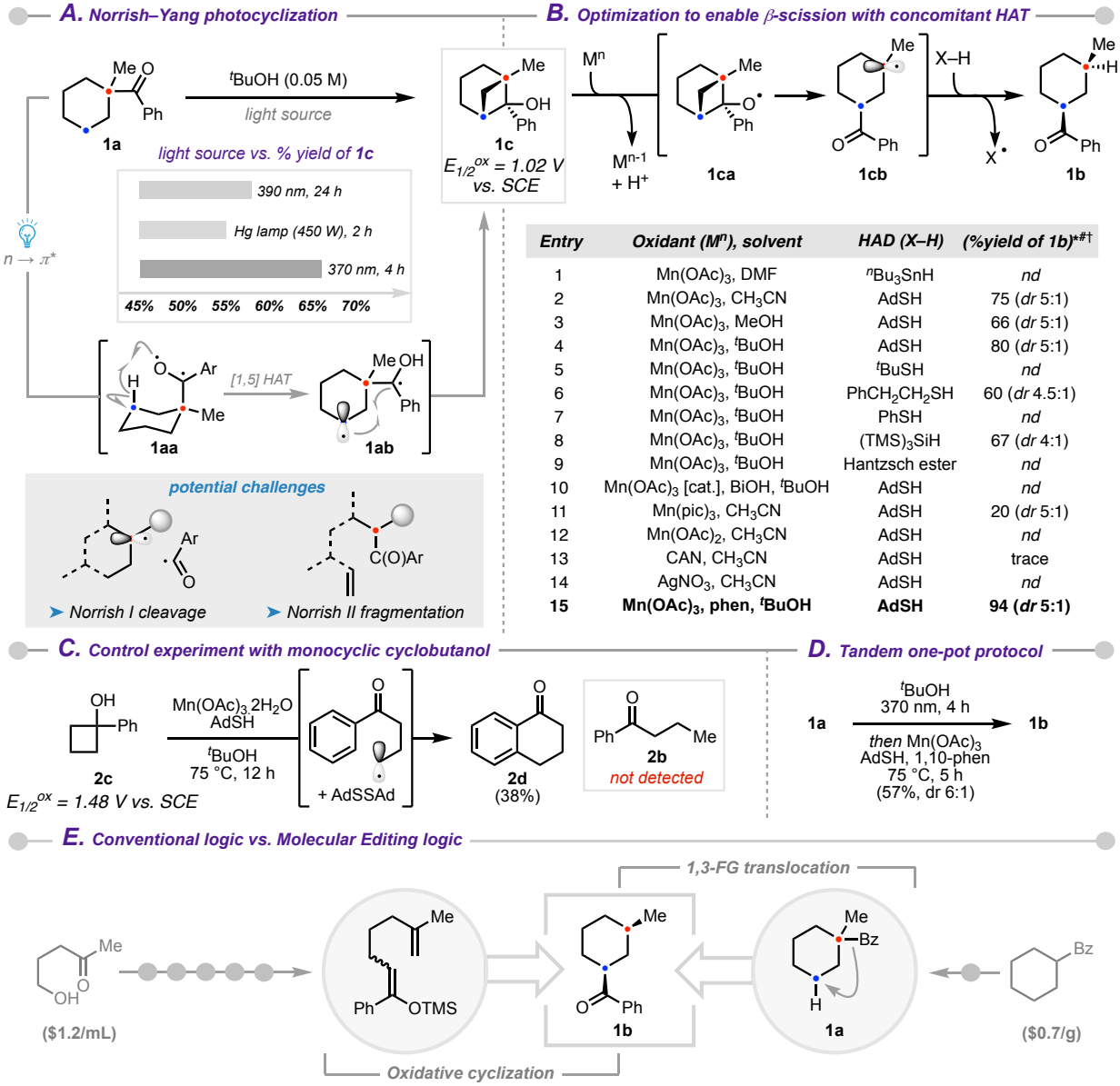

Fig. 2. Reaction development and optimization. (**A**) Proposed reaction mechanism and optimization studies of the targeted transannular Norrish–Yang photocyclization. (**B**) Establishment of optimal conditions to promote the desired β-scission accompanied by hydrogen-atom trapping. (**C**) Control experiment using a monocyclic cyclobutanol substrate. (**D**) Tandem one-pot reaction sequence. (**E**) Comparison of the conventional cyclization sequence with the translocation approach leading to product **1b**. *Yields refer to isolated yields after column chromatography. # In all cases, the diastereomeric ratio (*dr*) of **1b** was determined by ^{1}H NMR analysis of the crude reaction mixture, favoring the *cis*-isomer. †All optimization experiments were conducted on a 0.05-0.2 mmol scale; *nd*, not detected.

With access to **1c**, we next explored the generation of the oxygen-centered radical to trigger β-scission. Traditional approaches rely on pre-functionalization of alcohols to form weaker O–X bonds, facilitating radical formation. Alternative strategies include transition metal or photoredox-mediated oxidation, as well as redox-neutral processes such as proton-coupled electron transfer (PCET) or ligand-to-metal charge transfer (LMCT)[31,32]. However, only a few reports address β-scission with concurrent hydrogen-atom trapping[33,34]. To develop a practical, broadly applicable protocol free of expensive catalysts and forcing conditions, we examined other potential opportunities to promote the β-scission. Cyclic voltammetry (CV) revealed a low oxidation potential (1.02 V vs. SCE) of **1c**, likely due to inherent ring strain, suggesting the feasibility of selective oxidation in the presence of suitable hydrogen atom donors (HADs). Manganese-based single-electron oxidants are recognized for mild reactivity, sustainability, low toxicity, and have been employed to promote β-scission of cyclobutanols[35]. Inspired by this, we treated **1c** with manganese(III) acetate [$Mn(OAc)_3$, $Mn^{III/II}$: $E_{1/2}^0$ = 1.51 V vs. SCE][36] under thermal conditions in the presence of various HADs (Fig. 2B, entries 1–9). Among those tested, adamantane thiol ($E_{1/2}^{ox}$ = 1.34 V vs. SCE) proved optimal in *tert*-butanol (entry 4). Optimal efficiency required 3 equivalents of $Mn(OAc)_3$, which ensured complete consumption of **1c** while minimizing product decomposition. Lower loadings left unreacted substrate, accompanied by product decomposition under prolonged reaction times. Attempts to regenerate $Mn(OAc)_3$ catalytically or to use alternative oxidants were less successful (entries 10–14). Inclusion of 1,10-phenanthroline further optimized the conditions, yielding product **1b** in 94% (entry 15).

The success of the protocol derives from the unusually low oxidation potential of bicyclic intermediate **1c**, which enables selective oxidation without premature consumption of the thiol. In contrast, monocyclic cyclobutanol **2c** ($E_{1/2}^{ox}$ = 1.48 V vs. SCE) failed to furnish the corresponding linear ketone **2b**; instead, only tetralone **2d**[37] was isolated in 38% yield (Fig. 2C), and the thiol was fully oxidized to disulfide. The higher oxidation potential of **2c** relative to adamantane thiol precludes productive radical trapping. Collectively, the facile oxidizability of **1c** allows the thiol to persist in its reduced form and function effectively as a hydrogen atom donor under oxidative conditions. Recognition of this distinctive reactivity of **1c** proved essential to the successful implementation of the transformation via an unprecedented oxidative pathway. Notably, the entire sequence could be conducted in a tandem single-pot operation, enabling direct conversion of **1a** to **1b** in comparable overall yield (Fig. 2D). Using the one-pot translocation strategy, compound **1b** can be accessed from commercially available cyclohexyl phenyl ketone in two steps (Fig. 2E). By comparison, the conventional cyclization sequence[38] requires six steps starting from an acyclic alcohol, underscoring the marked improvement in step economy enabled by this translocation-based approach.

With the optimized conditions in hand, we evaluated the scope of the one-pot 1,3-translocation process (Fig. 3A). The method is practical due to the straightforward preparation of 1,1-disubstituted cyclohexyl substrates. A series of cyclohexyl derivatives bearing sterically diverse α-alkyl groups adjacent to the benzoyl moiety was synthesized, and the corresponding translocated products **1b** and **3b**–**6b** were obtained in moderate to good yields. The highest yield (80%) was observed for the substrate containing the bulkiest isopropyl group. The structure of **6b** was confirmed by X-ray crystallography of the corresponding DNP adduct (see Supplementary Information, Section 14.1), supporting the hypothesis that sterically hindered conformers adopt an

axial benzoyl orientation (**7**), aligning the diradical intermediate with C3 axial C–H bonds and facilitating the subsequent [1,5]-HAT.

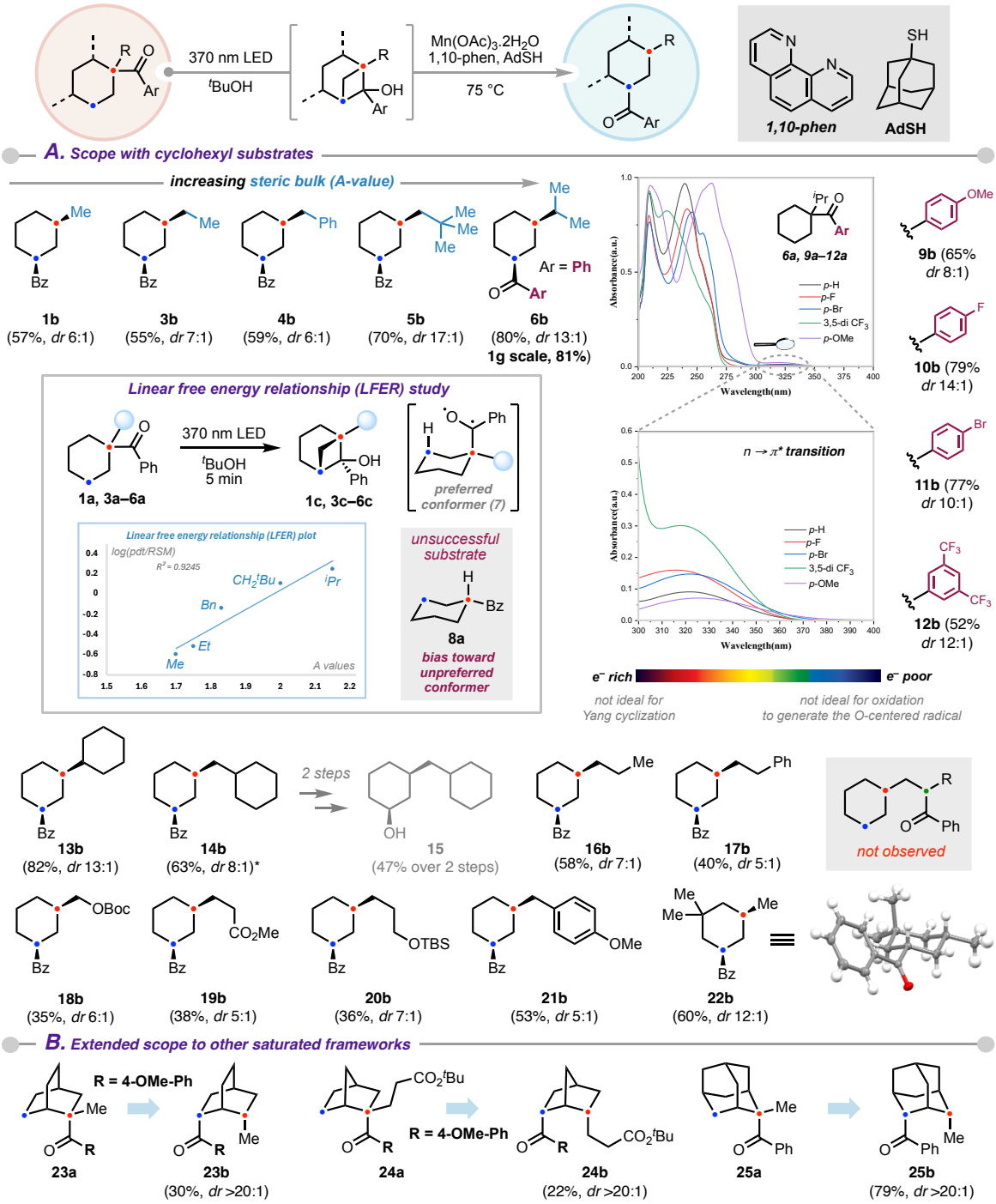

Fig. 3. Substrate Scope for 1,3-aroyl translocation. General reaction conditions: starting material (0.2-0.5 mmol) in ^{t}BuOH (0.05 M) under 370 nm LED irradiation for 2–4 h, followed by $Mn(OAc)_3.2H_2O$ (3.0 equiv), 1,10-phen (3.3 equiv), and AdSH (1.5 equiv), at 75 °C, 30 min to 6 h. Isolated yields are reported (*represents NMR yield), and relative stereochemistry is indicated. (**A**) Cyclohexyl substrate scope, evaluating the influence of steric variation at the α-substituent and the electronic nature of the aroyl group. (**B**) Scope extension to other saturated frameworks. Conditions for the Liner free energy relationship study: starting material (0.1 mmol) in ^{t}BuOH (0.05 M) under 370 nm LED irradiation for 5 min. UV-visible absorption spectra were recorded for substrate solutions in ^{t}BuOH.

To further probe this steric effect, a linear free energy relationship (LFER) study was conducted[39]. Substrates **1a** and **3a**–**6a** were irradiated under photocyclization conditions with truncated reaction times to preserve quantitative mass balance. The logarithm of the conversion ratio (product/RSM) correlated linearly ($R^2 = 0.92$) with the A-value[40] of the α-substituents, indicating that geometric alignment in the short-lived diradical **7** is critical for channeling the Norrish–Yang pathway. Substrates lacking an α-substituent (e.g., **8a**) failed to undergo Norrish–Yang cyclization and instead produced complex mixtures dominated by fragmentation, highlighting the importance of steric bias in directing the reaction. The scalability of the protocol was demonstrated by the gram-scale synthesis of **6b** without loss of yield.

We next explored the influence of electronic effects on the aroyl group. Substrates **9a**–**12a** bearing electron-donating (–OMe) and electron-withdrawing (–F, –Br, $–CF_3$) substituents were synthesized. While *p*-F and *p*-Br derivatives afforded products **10b** and **11b** in yields comparable to **6b**, electron-rich –OMe and electron-deficient $–CF_3$ substrates gave lower yields. UV–vis spectroscopy of **6a**, **9a**–**12a** revealed that $\pi \rightarrow \pi^*$ transitions are strongly modulated by electronic substitution, whereas $n \rightarrow \pi^*$ transitions were minimally affected. Thus, diminished yields for **9b** and **12b** likely arise from competing red-shifted $\pi \rightarrow \pi^*$ excitation in electron-rich substrates and reduced efficiency of oxidation to generate the oxygen-centered radical in electron-poor systems.

Expanding steric and functional-group tolerance, bulky α-cyclohexyl substitution provided **13b** in 82% yield, whereas a homologated cyclohexyl fragment (*less steric bias*) gave **14b** in 63%. The benzoyl group proved synthetically versatile: **14b** was converted to alcohol **15** via Baeyer–Villiger oxidation followed by hydrolysis, demonstrating its utility as a masked hydroxy equivalent. Linear alkyl–substituted substrates also underwent translocation, delivering **16b** and **17b**. Notably, substrates bearing alkyl chains with competing Cγ–H bonds showed no migration outside the ring, highlighting the strong preference for transannular migration in cyclohexyl systems. Carbonate, ester, silyl ether, and electron-rich aryl functionalities were tolerated, affording **18b**–**21b**. A geminal dimethyl substitution at one C3 position directed translocation to the remaining C3 site, yielding **22b** in 60%; its structure was confirmed by X-ray crystallography. Importantly, the protocol extends beyond simple cyclohexyl systems. Translocation was achieved in [2.2.2]- and [2.2.1]-bicyclic frameworks, yielding **23b** and **24b** in 30% and 22% yields, respectively, and in a rigid tricyclic adamantyl system to give **25b** in 79%, all exclusively favoring one diastereomer. The high diastereoselectivity likely reflects kinetic preference during the HAT step, while the success in the adamantyl system is attributed to its inherent symmetry in differentiating axial versus equatorial positions.

We next explored alternative electronic triggers to enable 1,3-translocation within the cyclization–cleavage decoupled framework. We hypothesized that substrates bearing an α-electron-withdrawing group would undergo Norrish–Yang cyclization to form an intermediate predisposed to retro-aldol–type ring opening, thereby relocating the aroyl group to C3 (Fig. 4A). Consistent with this design, irradiation of α-ester substrate **26a** followed by triethylamine treatment delivered translocated product **26b**. Notably, *cis*-**26b** had previously required a four-step sequence from isophthalic acid (**27**), underscoring the step economy of the present approach[41]. Isoquinoline-containing aroyl substrates were also compatible, yielding **28b**. In the adamantyl series, nitrile substituents similarly promoted translocation, producing **29b″** and **29b′** in a 3:1 ratio.

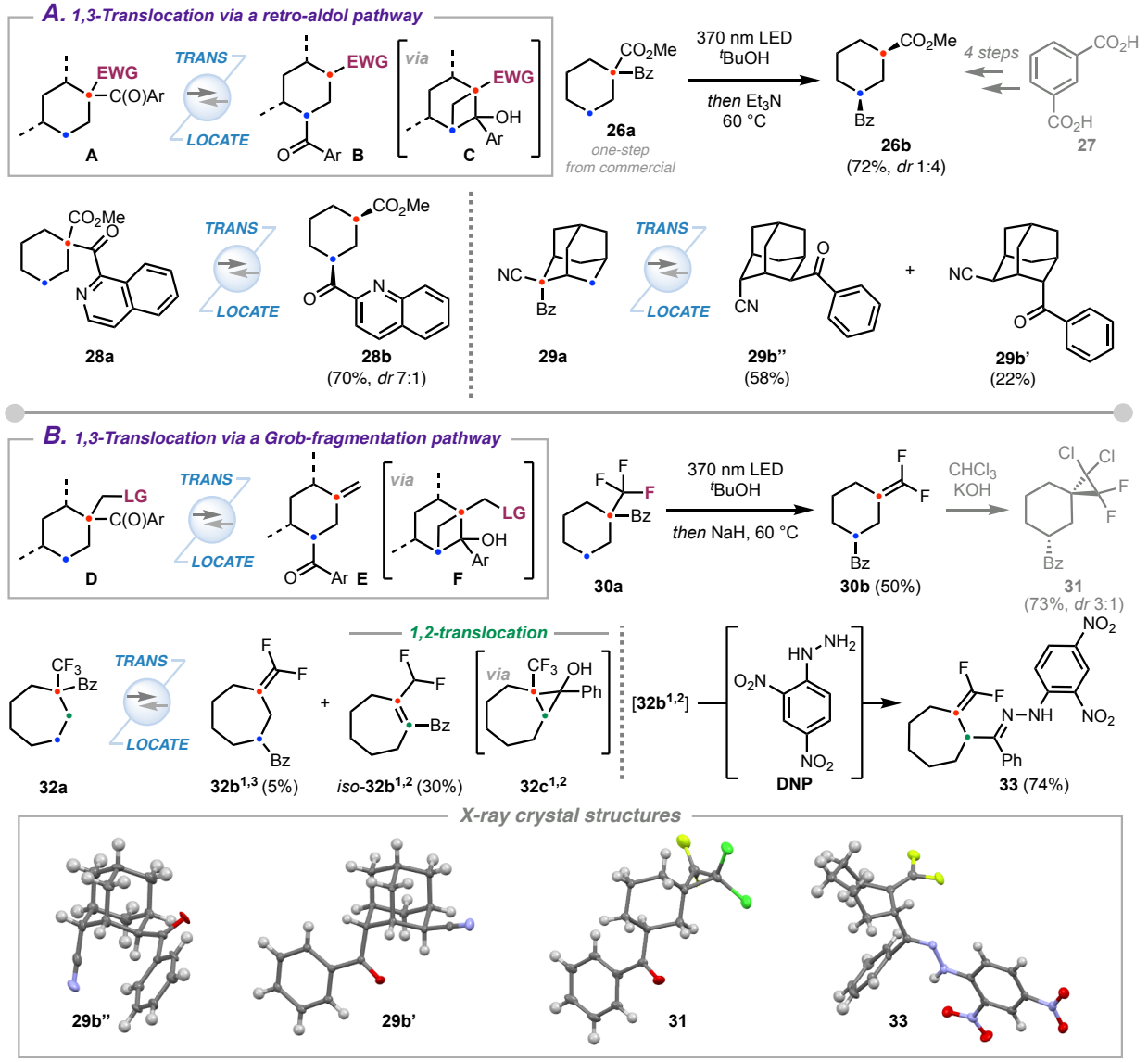

Fig. 4. Alternate pathways for achieving 1,3-aroyl translocation. (**A**) 1,3-Translocation proceeding via a retro-aldol-mediated pathway. Reaction conditions: starting material (0.2-0.5 mmol) in ^{t}BuOH (0.05 M), irradiation with a 370 nm LED for 2–4 h, followed by Et_3N (3.0 equiv) at 75 °C for 2–12 h. (**B**) 1,3-Translocation proceeding via a Grob-fragmentation pathway. Reaction conditions: starting material (0.2-0.5 mmol) in ^{t}BuOH (0.05 M), irradiation with a 370 nm LED for 2–4 h, followed by NaH (3.0 equiv) at 75 °C for 30 min to 4 h. Isolated yields are reported, and relative stereochemistry is indicated.

We further envisioned that α-substituted substrates bearing an appropriate leaving group could undergo a complementary Grob-type fragmentation[42] following photocyclization, enabling translocation while unveiling a substituted exomethylene unit at the parent position. Substrate **30a**, featuring an α-CF_3 group, underwent photocyclization and, upon treatment with NaH, underwent Grob fragmentation to furnish **30b**. The resulting difluoromethylene motif[43]—an established carbonyl bioisostere[44]—was leveraged in a subsequent cyclopropanation to deliver polyhalogenated spirocycle **31**. In cycloheptyl derivatives, increased conformational flexibility afforded both 1,2- (*iso*-**32b**^{1,2}) and 1,3- (**32b**^{1,3}) translocated products. Heating under basic conditions favored the conjugated 1,2-isomer *iso*-**32b**^{1,2}. The structure of **32b**^{1,2} was confirmed via

derivatization to DNP adduct **33** and subsequent X-ray crystallographic analysis. The observed 1,2-selectivity reflects altered Norrish–Yang cyclization selectivity in flexible systems, illustrating that the strategy can extend beyond 1,3-translocation. Collectively, these results demonstrate broad applicability and tunable selectivity of the one-pot translocation platform, enabled by pairing Norrish–Yang photocyclization with either radical-mediated β-scission or base-promoted ring-opening/fragmentation. Structures of **29b″**, **29b′**, **31**, and **33** were confirmed by single-crystal X-ray diffraction.

To demonstrate broader utility, we assessed the generality of 1,3-translocation across diverse synthetic platforms. First, we targeted a two-atom ring expansion of tetralone **34a** to access medium-sized ring system **34b** (Fig. 5A). Norrish–Yang cyclization delivered fused cyclobutanol **34c**; however, $Mn(OAc)_3$-mediated cleavage failed, consistent with the high oxidation potential (2.1 V vs. SCE) of **34c**. Using Knowles' PCET conditions[33], the desired β-scission was achieved, and the eight-membered product **34b** was obtained in 85% yield. Notably, an analogous expansion (**35a** → **35b**) is disfavored under Dowd–Beckwith conditions due to the kinetic instability of the corresponding radical intermediate **35c**[45], underscoring the importance of decoupling cyclization and cleavage and enabling ring expansion via a neutral cyclobutanol intermediate. Scaffold reorganization was also realized with spiro substrate **36a**, which underwent 1,3-translocation to generate a new bicyclic linkage in **36b**, thus rapidly increasing molecular complexity and incorporating a ten-membered ring (Fig. 5B).

An iterative translocation strategy was next explored to enable distal functionalization within a saturated framework (Fig. 5C). Substrate **6b**, obtained from **6a** via an initial translocation, was converted in two steps to trifluoromethylated precursor **37a**. Upon irradiation, the resulting oxygen-centered radical selectively engaged in [1,5]-HAT with the tertiary C–H bond adjacent to the isopropyl substituent, and upon basic treatment restored the benzoyl group to its original position (*second translocation*) while installing a difluoromethylene unit at C3 site. This provided C3-functionalized product **37b″** via two sequential translocations from **6a**; trace formation of product **37b′** was observed from competing migration to the alternate C3 position. Finally, the stereospecificity of the translocation was demonstrated using chiral substrates (Fig. 5D). Enantiopure **38a**, derived from (+)-camphoric acid, underwent stereospecific translocation via **38c**, desymmetrizing a gem-dimethyl unit and furnishing a cyclopentyl framework bearing three contiguous stereocenters. Similarly, (+)-dihydrocarvone-derived **39a** produced diastereomers **39b** and *epi*-**39b** in 51% and 30% yield, respectively[46].

The high regioselectivity of aroyl translocation mirrors the selectivity of the hydrogen atom transfer (HAT) event in the Norrish–Yang cyclization. For cyclohexyl substrates, intra-ring translocation is exclusively favored, despite competing Cγ–H bonds on appended alkyl chains. To elucidate this bias, DFT calculations were performed at the CAM-B3LYP/6-31+G(d,p) level with GD3BJ dispersion corrections[47]. In the triplet state of **16a**, the oxygen-centered radical is significantly closer to the intra-ring Cγ–H bond than to the alkyl-chain Cγ–H bond (2.39 Å vs. 2.75 Å), resulting in a substantially lower activation barrier for intra-ring HAT via **TSb**. This geometric preference accounts for the exclusive formation of the transannular product.

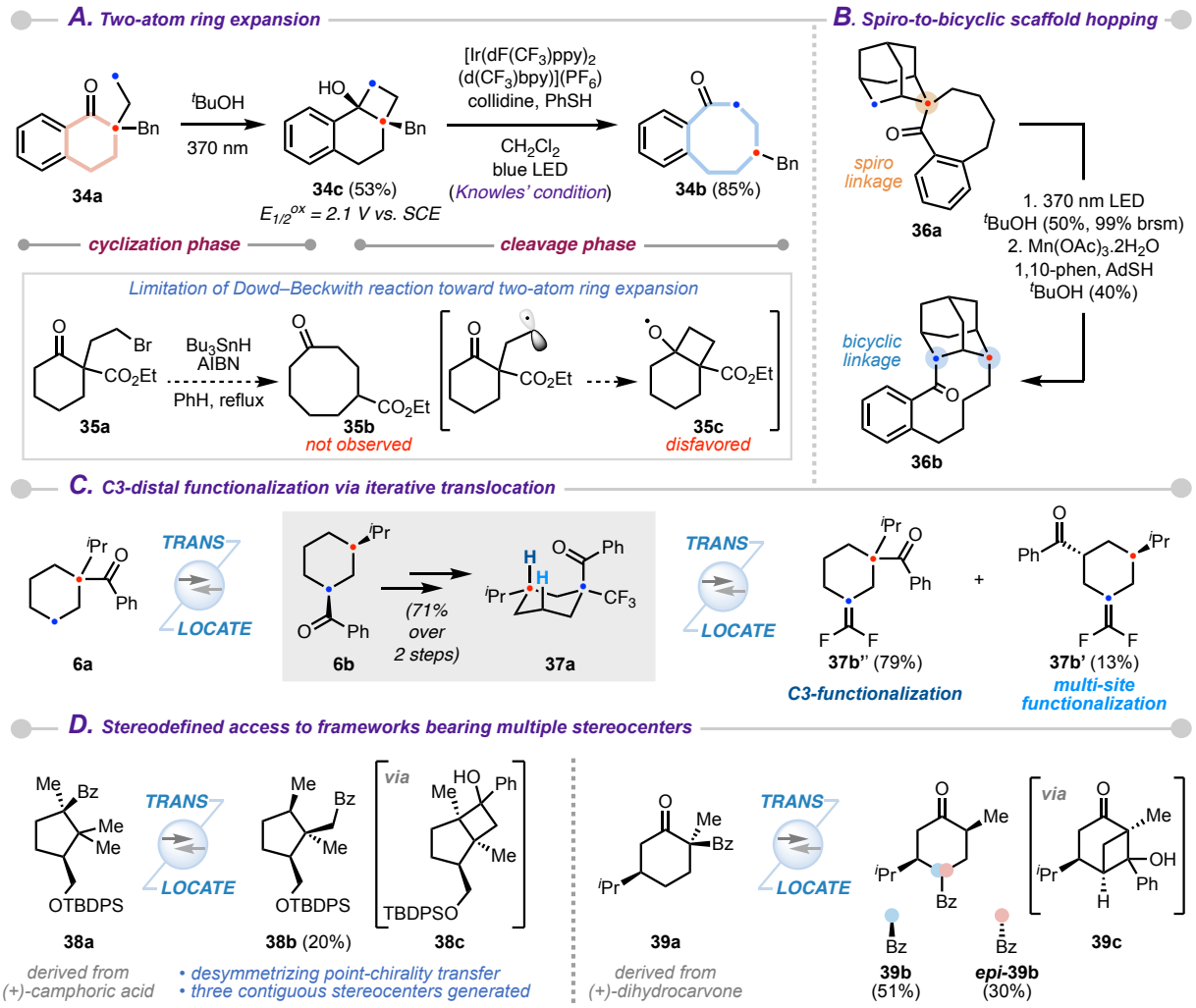

Fig. 5. Synthetic applications of the 1,3-aroyl translocation. (**A**) Two-atom ring expansion strategy. (**B**) A scaffold hopping protocol to translate a spiro linkage in the substrate to a bicyclic linkage in the product. (**C**) Distal-functionalization enabled through iterative translocation. (**D**) Efficient access to stereodefined frameworks bearing multiple stereocenters. All reactions were conducted on a 0.2-0.5 mmol scale.

To probe radical intermediacy in the translocation step, we attempted trapping of the putative tertiary radical. Treatment of Norrish–Yang intermediate **1c** with $Mn(OAc)_3$ in the presence of TEMPO afforded TEMPO adduct **40** as a 2:1 mixture of diastereomers. Reductive N–O bond cleavage with Zn under acidic conditions delivered tertiary alcohol **41**. This sequence not only supports radical involvement but also reveals a new translocative hydroxylation manifold, in which aroyl group migration is coupled with the installation of a hydroxy group at the original site. Consistent with this concept, substrates **42** and **25a** underwent analogous transformations to yield products **43** and **44**, featuring aroyl migration to C3 alongside hydroxylation at C1. The excellent diastereoselectivity observed for **44** further highlights the stereospecific nature of the translocation and the intrinsic bias governing TEMPO capture.

As a control, treatment of **1c** with $Mn(OAc)_3$ alone in the absence of a radical trap produced a mixture of olefins **45′–45‴** in a 1:1.2:1.2 ratio, consistent with the intermediacy of a tertiary carbocation (**45-int**) via oxidation of the radical intermediate. These observations support the

coexistence of radical and ionic pathways, dictated by the reaction conditions. This dual mechanistic manifold was further illustrated using substrate **46**: standard conditions delivered the translocated product (**47**) selectively, whereas omission of a radical trap led to spiro-lactone **48**, arising from an oxidative radical–polar crossover via carbocation **48-int**[48]. These findings demonstrate that $Mn(OAc)_3$ can access divergent outcomes through controlled engagement of either radical or ionic intermediates.

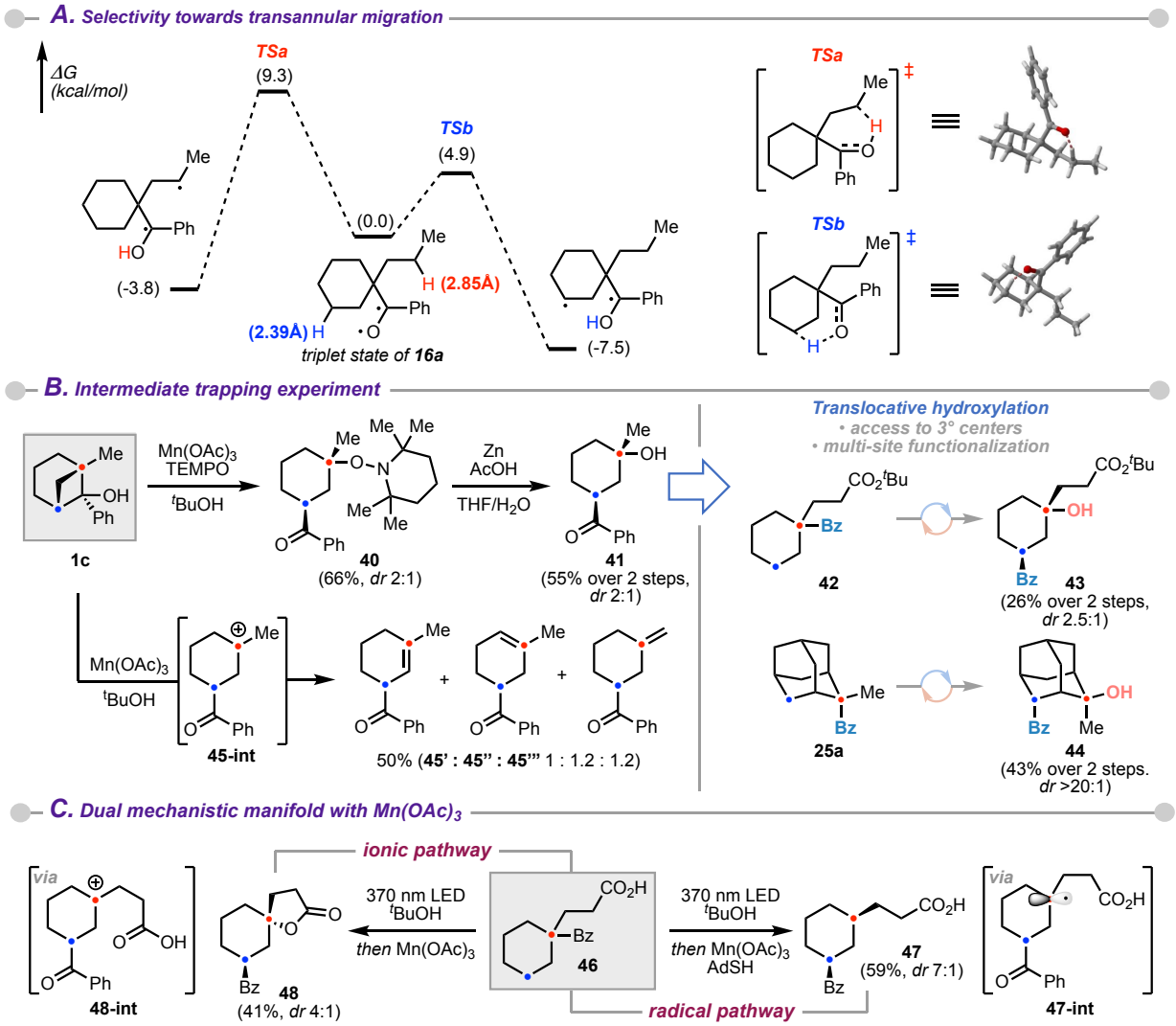

Fig. 6. Mechanistic studies. (**A**) Computational analysis supporting the experimentally observed selectivity for transannular migration. (B) Intermediate-trapping experiments that uncover a previously unexplored mode of translocative hydroxylation in saturated carbocyclic frameworks. (C) Evidence for a dual mechanistic manifold with $Mn(OAc)_3$. Density functional theory (DFT) calculations are detailed in Supplementary Information, Section 15.2.

In summary, we have developed a decoupled, position-controlled strategy that enables transannular migration of aroyl groups within saturated carbocyclic frameworks, providing direct access to otherwise elusive 1,3-disubstituted architectures. By decoupling Norrish–Yang photocyclization from downstream oxidative cleavage through a neutral bicyclic intermediate, this strategy circumvents kinetic limitations that have historically precluded 1,3-translocation and allows controlled skeletal reorganization under mild, operationally simple conditions. The unusual

compatibility of $Mn(OAc)_3$ as an oxidant with a thiol reductant—without mutual quenching—allows independent and programmable reactivity, unlocking both radical and ionic manifolds from a common intermediate. This design unlocks multiple mechanistic pathways and provides broad applicability across diverse saturated frameworks, delivering 1,3-disubstituted products with precise positional control. Beyond enabling 1,3-translocation, this platform offers a general blueprint for translocative functionalization on saturated scaffolds. Its broad substrate scope, stereospecificity, and adaptability support ring expansion, scaffold hopping, distal functionalization through iterative translocation, and precise editing of chiral molecules. Collectively, these features position this strategy as a powerful tool for three-dimensional molecular editing, with clear implications for drug discovery and the design of functional materials where spatial control of substituents is paramount.

References

1. Hui, C., Craggs, L., & Antonchick, A. P. Ring contraction in synthesis of functionalized carbocycles. *Chem. Soc. Rev.* **51**, 8652–8675 (2022).
2. Hu, Y. J., Li, L. X., Han, J. C., Min, L., & Li, C. C. Recent advances in the total synthesis of natural products containing eight-membered carbocycles (2009–2019). *Chem. Rev.* **120**, 5910–5953 (2020).
3. Ferreira, A. J. & Beaudry, C. M. Synthesis of natural products containing fully functionalized cyclopentanes. *Tetrahedron* **73**, 965–1084 (2017).
4. Ma, C., Lindsley, C. W., Chang, J. & Yu, B. Rational molecular editing: A new paradigm in drug discovery. *J. Med. Chem.* **67**, 11459–11466 (2024).
5. Steele, R. T., Fujiu, M. & Sarpong, R. 1,2-Acyl transposition through photochemical skeletal rearrangement of 2,3-dihydrobenzofurans. *Science* **388**, 631–638 (2025).
6. Wu, Z., Xu, X., Wang, J. & Dong, G. Carbonyl 1,2-transposition through triflate-mediated α-amination. *Science* **374**, 734–740 (2021).
7. Brägger, Y., Green, O., Bhawal, B. N. & Morandi, B. Late-stage molecular editing enabled by ketone chain-walking isomerization. *J. Am. Chem. Soc.* **145**, 19496–19502 (2023).
8. Studer, A. & Bossart, M. Radical aryl migration reactions. *Tetrahedron* **57**, 9649–9667 (2001).
9. Xie, L., Luo, P., Lu, T., Zheng, W., Su, Y., Wang, J., Qi, X. & Xu, Y. 1,2-Boryl/hydrogen transposition via reversible C–H sampling. *ChemRxiv* [Preprint] (2025). doi:10.26434/chemrxiv-2025-lx3t5
10. Zhang, W., Mao, S., Peng, M. & Xi, Y. Versatile positional editing of diverse functional groups through radical 1,2-boron shifts. *ChemRxiv* [Preprint] (2025). doi:10.26434/chemrxiv-2025-61whz.
11. Chen, K., Zeng, Q., Xie, L., Xue, Z., Wang, J. & Xu, Y. Functional-group translocation of cyano groups by reversible C–H sampling. *Nature* **620**, 1007–1012 (2023).
12. Han, W., Hwang, T., Lian, C., Kolb, S., Yamane, M., Palani, V. & Wendlandt, A. E. Migrating group strategy for remote functionalization of seven-membered rings. *J. Am. Chem. Soc.* **147**, 32077–32084 (2025).
13. Li, W., Xu, W., Xie, J., Yu, S. & Zhu, C. Distal radical migration strategy: An emerging synthetic means. *Chem. Soc. Rev.* **47**, 654–667 (2018).

14. Grover, J., Sebastian, A. T., Maiti, S., Bissember, A. C., & Maiti, D. Unified approaches in transition metal catalyzed C(sp^3)-H functionalization: recent advances and mechanistic aspects. *Chem. Soc. Rev.* **54**, 2006–2053 (2025).
15. Gao, Y., & Ma, D. In pursuit of synthetic efficiency: Convergent approaches. *Acc. Chem. Res.* **54**, 569–582 (2021).
16. Tang, K., Wang, S., Gao, W., Song, Y., & Yu, B. Harnessing the cyclization strategy for new drug discovery. *Acta Pharm. Sin. B.* **12**, 4309–4326 (2022).
17. Kang, G., Strassfeld, D. A., Sheng, T., Chen, C. Y., & Yu, J. Q. Transannular C–H functionalization of cycloalkane carboxylic acids. *Nature* **618**, 519–525 (2023).
18. Abrams, D. J., Provencher, P. A., & Sorensen, E. J. Recent applications of C–H functionalization in complex natural product synthesis. *Chem. Soc. Rev.* **47**, 8925–8967 (2018).
19. Godula, K. & Sames, D. C-H Bond functionalization in complex organic synthesis. *Science* **312**, 67–72 (2006).
20. La, D. S., Salituro, F. G., Botella, G. M., Griffin, A. M., Bai, Z., Ackley, M. A., Dai, J., Doherty, J. J., Harrison, B. L., Hoffmann, E. C., Kazdoba, T. M., Lewis, M. C., Quirk, M. C. & Robichaud, A. J. Neuroactive steroid *N*-methyl-D-aspartate receptor positive allosteric modulators: Synthesis, SAR, and pharmacological activity. *J. Med. Chem.* **62**, 7526–7542 (2019).
21. Ishikawa, M., Hiraiwa, Y., Kubota, D., Tsushima, M., Watanabe, T., Murakami, S., Ouchi, S. & Ajito, K. Tricyclic pharmacophore-based molecules as novel integrin $\alpha_v\beta_3$ antagonists. Part III: Synthesis of potent antagonists with $\alpha_v\beta_3/\alpha_{IIb}\beta_3$ dual activity and improved water solubility, *Bioorg. Med. Chem.* **14**, 2131–2150 (2006).
22. Xu, Y., Wu, Z., Jiang, J., Ke, Z. & Zhu, C. Merging distal alkynyl migration and photoredox catalysis for radical trifluoromethylative alkynylation of unactivated olefins. *Angew. Chem. Int. Ed.* **56**, 4545–4548 (2017).
23. Wu, Z., Ren, R. & Zhu, C. Combination of a cyano migration strategy and alkene difunctionalization: The elusive selective azidocyanation of unactivated olefins. *Angew. Chem. Int. Ed.* **55**, 10821–10824 (2016).
24. Yang, N. C. & Yang, D. D. H. Photochemical reactions of ketones in solution. *J. Am. Chem. Soc.* **80**, 2913–2914 (1958).
25. Poudrel, J. M., Hullot, P., Vidal, J. P., Girard, J. P., Rossi, J. C., Muller, A., Bonne, C., Bezuglov, V., Serkov, I., Renard, P. & Pfeiffer, B. Synthesis and structure–activity relationships of new 1,3-disubstituted cyclohexanes as structurally rigid leukotriene B_4 receptor antagonists. *J. Med. Chem.* **42**, 5289–5310 (1999).
26. McMinn, D. & Rao, M. Thiazole derivatives as protein secretion inhibitors. Patent WO 2020/176863 A1 (3 September 2020).
27. Nakahara, H., Isshiki, R., Kubo, M., Iizumi, K., Muto, K. & Yamaguchi, J. Versatile deacylative cross-coupling of aromatic ketones. *Chem* **10**, 2916–2930 (2024).
28. Chaudhary, A. G., Chordia, M. D. & Kingston, D. G. I. A novel benzoyl group migration: Synthesis and biological evaluation of 1-benzoyl-2-des(benzoyloxy)paclitaxel. *J. Org. Chem.* **60**, 3260–3262 (1995).
29. Lewis, F. D., Johnson, R. W. & Johnson, D. E. Conformational control of photochemical behavior. Competitive α-cleavage and γ-hydrogen abstraction of alkyl phenyl ketones. *J. Am. Chem. Soc.* **96**, 6090–6099 (1974).

30. Xia, W., Scheffer, J. R., Botoshansky, M. & Kaftory, M. Photochemistry of 1-isopropylcycloalkyl aryl ketones: Ring size effects, medium effects, and asymmetric induction. *Org. Lett.* **7**, 1315–1318 (2005).
31. Chang, L., An, Q., Duan, L., Feng, K. & Zuo, Z. Alkoxy radicals see the light: New paradigms of photochemical synthesis. *Chem. Rev.* **122**, 2429–2486 (2022).
32. Tsui, E., Wang, H. & Knowles, R. R. Catalytic generation of alkoxy radicals from unfunctionalized alcohols. *Chem. Sci.* **11**, 11124–11141 (2020).
33. Yayla, H. G., Wang, H., Tarantino, K. T., Orbe, H. S. & Knowles, R. R. Catalytic ring-opening of cyclic alcohols enabled by PCET activation of strong O–H bonds. *J. Am. Chem. Soc.* **138**, 10794–10797 (2016).
34. Liu, W., Wu, Q., Wang, M., Huang, Y. & Hu, P. Iron-catalyzed C–C single-bond cleavage of alcohols. *Org. Lett.* **23**, 8413–8418 (2021).
35. Wu, X. & Zhu, C. Recent advances in ring-opening functionalization of cycloalkanols by C–C σ-bond cleavage. *Chem. Rec.* **18**, 587–598 (2018).
36. Wang, M., Wu, Z. & Zhu, C. Ring-opening selenation of cyclobutanoles: synthesis of γ-selenylated alkyl ketones through C–C bond cleavage. *Org. Chem. Front.* **4**, 427–430 (2017).
37. Petti, A., Natho, P., Lam, K. & Parsons, P. J. Regioselective electrochemical cyclobutanol ring expansion to 1-tetralones. *Eur. J. Org. Chem.* **2021**, 854–858 (2021).
38. Ackermann, L., Heidbreder, A., Wurche, F., Klärner, F. G. & Mattay, J. Mechanistic studies on PET-oxidative cyclization of unsaturated silyl enol ethers: dependence of the regioselectivity on alcohol addition and pressure effects. *J. Chem. Soc., Perkin Trans.* **2**, 863–870 (1999).
39. Wells, P. R. Linear free energy relationships. *Chem. Rev.* **63**, 171–219 (1963).
40. Muller, P. Glossary of terms used in physical organic chemistry (IUPAC Recommendations 1994). *Pure Appl. Chem.* **66**, 1077–1184 (1994).
41. Johnson, J. B., Cook, M. J. & Rovis, T. Ligand differentiated complementary Rh-catalyst systems for the enantioselective desymmetrization of *meso*-cyclic anhydrides. *Tetrahedron* **65**, 3202–3210 (2009).
42. Prantz, K. & Mulzer, J. Synthetic applications of the carbonyl generating Grob fragmentation. *Chem. Rev.* **110**, 3741–3766 (2010).
43. Sap, J. B. I., Meyer, C. F., Straathof, N. J. W., Iwumene, N., Am Ende, C. W., Trabanco, A. A. & Gouverneur, V. Late-stage difluoromethylation: concepts, developments and perspective. *Chem. Soc. Rev.* **50**, 8214–8247 (2021).
44. Zhang, M., Luo, M. & Wang, H. Catalytic asymmetric synthesis of vicinal chiral carbonyl bioisoteres. *Eur. J. Org. Chem.* [Early View] (2025). doi: org/10.1002/ejoc.202501098.
45. Dowd, P. & Choi, S. C. Free radical ring expansion by three and four carbons. *J. Am. Chem. Soc.* **109**, 6548–6549 (1987).
46. Hasegawa, T., Nishimura, M., Kodama, Y. & Yoshioka, M. Photochemical reaction of 1,3-diketones. Transformation of 2-benzoyl-2-methylcyclohexanones to 4-benzoyl-2-methylcyclohexanones. *Bull. Chem. Soc. Jpn.* **63**, 935–937 (1990).
47. Sang, J., Orimoto, Y. & Aoki, Y. Theoretical analysis of the Norrish reaction mechanism in aliphatic polyamide. *Phys. Chem. Chem. Phys.* **27**, 15787–15802 (2025).
48. Snider, B. B. Manganese (III)-based oxidative free-radical cyclizations. *Chem. Rev.* **96**, 339–364 (1996).

Acknowledgements: We thank Dr. G. Jindal (IISc) for guidance on computational studies and Dr. S. Kumar (IISc) for CV and UV data acquisition and analysis. We acknowledge Mr. Shashikant J. (IISc) for X-ray crystallographic studies. We are grateful to Mr. P. Mukherjee (IISc), Mr. S. Selvaraj (IISc), and Ms. S. Banerjee (IISER Bhopal) for assistance in synthesizing select substrates. High-resolution mass spectra (HR-MS) were recorded using instrumentation procured under the Department of Science and Technology (DST)-FIST grant [SR/FST/CS II-040/2015]. V.P. thanks IISc for the start-up grant (IE/CARE-23-0318 and IE/RERE-23-0535) and infrastructure support. V.P. acknowledges additional funding from Anusudhan National Research Foundation (ANRF/ECRG/2024/000644/CS) and DST-INSPIRE (DST/INSPIRE/04/2023/000023). L.H.R. thanks the Council of Scientific and Industrial Research (09/0079(17043)/2023-EMR-I) for financial support. D.N. is grateful to IISc for a doctoral fellowship.

Authors contributions: V.P. designed the project and wrote the original draft of the manuscript. L.H.R. and D.N. conducted the main experiments and prepared the Supplementary Information. J.G. prepared some substrates and performed the DFT calculations. All authors contributed to assembling the final draft of the manuscript.

Competing interests: The authors declare that they have no competing interests.

Supplementary Information
Materials and Methods
Supplementary Text
Figures S1 to S36
Tables S1 to S14
References (1–47)

Data availability: X-ray crystallographic data for compounds **S97** (CCDC 2524430), **22b** (CCDC 2522864), **29b''** (CCDC 2520375), **29b'** (CCDC 2520376), **31** (CCDC 2523492), and **33** (CCDC 2520374) are available from the Cambridge Crystallographic Data Centre (https://www.ccdc.cam.ac.uk/). All other data are available in the main text or the supplementary Information.

Correspondence and requests for materials should be addressed to Vignesh Palani.